ELSEVIER

Carbohydrate Research 337 (2002) 409–420

CARBOHYDRATE RESEARCH

www.elsevier.com/locate/carres

Structural analysis of lipopolysaccharide oligosaccharide epitopes expressed by non-typeable *Haemophilus influenzae* strain 176

Elke K.H. Schweda,[a,*] Jianjun Li,[b] E. Richard Moxon,[c] James C. Richards[b]

[a]*Clinical Research Centre, Karolinska Institutet and University College of South Stockholm, NOVUM, S-141 86 Huddinge, Sweden*
[b]*Institute for Biological Sciences, National Research Council of Canada, Ottawa, Ont., Canada K1A OR6*
[c]*Molecular Infectious Diseases Group, Department of Pediatrics, University of Oxford, Weatherall Institute of Molecular Medicine, John Radcliffe Hospital, Headington, Oxford 0X3 9DS, UK*

Received 20 August 2001; received in revised form 29 November 2001; accepted 20 December 2001

Abstract

The structure of the lipopolysaccharide (LPS) from non-typeable *Haemophilus influenzae* strain 176 has been investigated. Electrospray ionization-mass spectrometry (ESIMS) on *O*-deacylated LPS (LPS-OH) and core oligosaccharide (OS) samples obtained after mild-acid hydrolysis of LPS provided information on the composition and relative abundance of the glycoforms. ESIMS tandem-mass spectrometry on LPS-OH confirmed the presence of minor sialylated and disialylated glycoforms. Oligosaccharide samples were studied in detail using high-field NMR techniques. It was found that the LPS contains the common inner-core element of *H. influenzae*, L-α-D-Hep*p*-(1→2)-[*P*Etn→6]-L-α-D-Hep*p*-(1→3)-[β-D-Glc*p*-(1→4)]-L-α-D-Hep*p*-(1→5)-[*PP*Etn→4]-α-Kdo*p*-(2→6)-Lipid A having glycosyl substitution at the O-3 position of the terminal heptose as recently observed for non-typeable *H. influenzae* strain 486 [Månsson, M.; Bauer, S. H. J.; Hood, D. W.; Richards, J. C.; Moxon, E. R.; Schweda, E. K. H., *Eur. J. Biochem.* **2001**, *268*, 2148–2159]. The following LPS structures were identified as the major glycoforms, the most significant being indicated with an asterisk (*) (glycoforms are partly substituted with Gly at the terminal Hep):

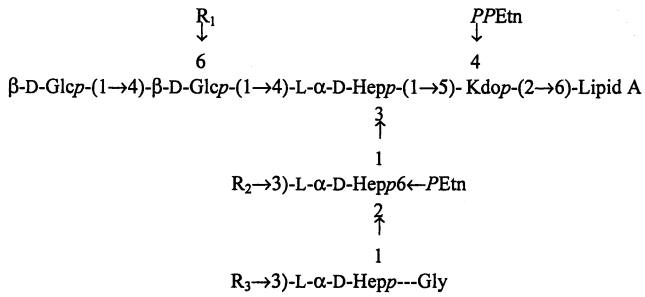

* R_1= *P*Cho, R_2= OH, R_3= β-D-Gal*p*(1;

* R_1= OH, R_2= α-D-Glc*p*-(1, R_3= β-D-Gal*p*(1;

R_1= *P*Cho, R_2= OH, R_3= OH;

R_1= OH, R_2= α-D-Glc*p*-(1, R_3= OH.

Keywords: Haemophilus; Lipopolysaccharide; Phosphocholine; 5-*N*-Acetylneuraminic acid; CE-ESIMS/MS

Abbreviations: LPS, lipopolysaccharide; LPS-OH, *O*-deacylated LPS; Lipid A-OH, *O*-deacylated lipid A; Kdo, 3-deoxy-D-*manno*-oct-2-ulosonic acid; *An*Kdo-ol, reduced anhydro Kdo; Hep, L-*glycero*-D-*manno*-heptose; Hex, hexose; HexNAc, *N*-acetylhexosamine; Neu5Ac, 5-*N*-acetylneuraminic acid; *P*Cho, phosphocholine; *P*Etn, phosphoethanolamine; *PP*Etn, pyrophosphoethanolamine; NTHi, non-typeable *Haemophilus influenzae*; CE, capillary electrophoresis; MS/MS, tandem-mass spectrometry; HPAEC, high-performance anion-exchange chromatography.

* Corresponding author. Tel.: +46-8-58583823; fax: +46-8-58583820.
E-mail address: elke.schweda@kfc.ki.se (E.K.H. Schweda).

0008-6215/02/$ - see front matter © 2002 Elsevier Science Ltd. All rights reserved.
PII: S0008-6215(02)00002-2

1. Introduction

Diseases caused by *Haemophilus influenzae* remain a significant problem worldwide. Type b capsular strains are associated with invasive diseases, including meningitis and pneumonia, while acapsular or non-typeable strains of *H. influenzae* (NTHi) are primary pathogens in otitis media and respiratory tract infections. Lipopolysaccharide (LPS) is an essential and characteristic surface component of these pathogens and is implicated as a major virulence factor. LPS of *H. influenzae* can mimic host glycolipids and has a propensity for reversible switching of terminal epitopes (phase variation) of the oligosaccharide portion. The conserved part of LPS from *H. influenzae* has been found to consist of a triheptosyl inner-core moiety in which each of the heptose residues (designated HepI, HepII and HepIII) can provide a point for elongation by oligosaccharide chains or for attachment of non-carbohydrate substituents (Structure **1**).[1]

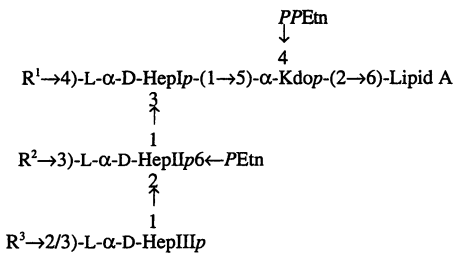

1 (R^1, R^2, R^3 = H or sugar residues)

To date, HepI has been found to be substituted by glucose (R_1 = β-D-Glc*p*) in all strains investigated. There is no chain extension from HepII in type d derived strain Rd, however, in three type b strains and NTHi strain 486, HepII is substituted by a glucose residue (R_2 = α-D-Glc*p*) which can provide a point for further chain extension. HepIII is substituted by galactose (R_3 = β-D-Gal*p*-(1→2); type b) or oligosaccharides extending from glucose (R_3 = β-D-Glc*p*-(1→2); Rd; R_3 = β-D-Glc*p*-(1→3); NTHi strain 486). Prominent non-carbohydrate substituents are phosphate (*P*), pyrophosphoethanolamine (*PP*Etn), phosphoethanolamine (*P*Etn), phosphocholine (*P*Cho), acetate (Ac) and glycine (Gly).

The oligosaccharide portion of *H. influenzae* LPS is known to be subject to high-frequency phase-variation of terminal epitopes, which can lead to a very heterogeneous population of LPS molecules within a single strain.[2] Phase variation is thought to provide an adaptive mechanism which is advantageous for survival of bacteria confronted by the differing microenvironments and immune responses of the host.[3,4] A genetic mechanism contributing to LPS phase-variation has been identified in five chromosomal loci; *lic*1, *lic*2, *lic*3, *lgtC* and *lex*2.[5–7] It has been demonstrated that expression of phosphocholine (*P*Cho) substituents in *H. influenzae* LPS is subject to phase variation mediated by genes in the *lic*1 locus.[8] Genes comprising the *lic*2 locus have been shown to be required for chain extension from HepII and, together with *lgtC*, in the phase variable expression of the p^k epitope [α-D-Gal*p*-(1→4)-β-D-Gal*p*-(1→4)-β-D-Glc*p*-(1→].[9–11] Recently, the first open reading frame in the *lic*3 locus was shown to encode an α-2,3-sialyltransferase that is responsible for addition of sialic acid (*N*-acetylneuraminic acid or Neu5Ac) to terminal lactose.[12] The phase-variable gene known as *lex*2 has been shown to encode a glucosyltransferase important in further oligosaccharide extension from HepI in the inner-core [Aubrey, R.; Hood, D. W.; Cox, A. D.; Makepeace, K.; Richards, J. C.; Moxon, E. R. unpublished]. The availability of the complete genome sequence of *H. influenzae* strain Rd has facilitated a comprehensive study of LPS biosynthetic loci in the type b strain Eagan (RM153) and in a homologous capsule deficient strain Rd^- (RM118).[10,13] Gene functions have been identified that are responsible for most of the steps in the biosynthesis of the oligosaccharide portion of the LPS molecules. Our ongoing studies have focussed on the structural diversity of LPS expression and the genetic basis for that diversity in a representative set of NTHi clinical isolates obtained from otitis media patients. In the present investigation we report on the structural analysis of LPS from one of these strains (NTHi strain 176) which provides the second example for a glycosyl substitution at O3 of HepIII (Structure **1**).

2. Results

Isolation and characterization of LPS.—H. influenzae non-typeable strain 176 is a clinical isolate gathered as part of a Finnish study of otitis media. The strain was grown in liquid culture and the LPS was isolated by phenol–chloroform–diethyl ether extraction. Compositional analysis of the LPS samples indicated D-glucose (Glc), D-galactose (Gal), 2-amino-2-deoxy-D-glucose (GlcN), and L-*glycero*-D-*manno*-heptose (Hep) as the constituent sugars (Glc:Gal:GlcN:Hep ratio of 1.0:0.6:0.3:1.0), which were identified by GLC–MS of the derived alditol acetates and 2-butyl glycoside derivatives. In addition, 5-*N*-acetylneuraminic acid (Neu5Ac) and glycine were detected as substituents of the LPS by high-performance anion-exchange chromatography (HPAEC).[14,15] Methylation analysis of LPS revealed the presence of terminal Glc, terminal Gal, 4-substituted Glc, 3-substituted Gal, 3-substituted-Hep, and 3,4-disubstituted Hep as the major sugar components in the relative proportions 22:17:7:6:19:22 (Table 1). After dephosphorylation of LPS with 48%

hydrogen fluoride, methylation analysis of the resulting material (LPS-*P*) showed terminal Glc, terminal Gal, 4-substituted Glc, 2-substituted Hep, 3-substituted-Hep, 3,4-disubstituted Hep, and 2,3-disubstituted Hep in the relative proportions 13:10:14:12:12:26:8 (Table 1). The appearance and increase of 2- and 2,3-substituted Hep after dephosphorylation was consistent with the LPS containing bi- and triantennary structures with the common conserved inner-core element, L-α-D-Hep*p*-(1→2)-L-α-D-Hep*p*-(1→3)-[β-D-Glc*p*-(1→4)-]-L-α-D-Hep*p*-(1→5)-α-Kdo of *H. influenzae* LPS (Structure **1**). The presence of this structural element was confirmed by subsequent ESIMS and NMR analysis (see below). The appearance of 3-substituted Hep indicated the alternate substitution pattern to HepIII (Structure **1**). In addition, the increase of 4-substituted Glc after dephosphorylation indicated this residue to be phosphorylated. It is noteworthy that 3-substituted Gal decreases significantly in the methylation analysis of LPS-*P*, possibly indicating a substitution of a Neu5Ac residue (see below).

O-Deacylation of LPS by treatment with anhydrous hydrazine under mild conditions afforded water-soluble material which was subjected to analysis by mass spectrometric techniques. The ESIMS spectrum of the sample (negative mode) revealed abundant molecular peaks corresponding to triply and quadruply deprotonated ions. The MS data (Table 2) pointed to the presence of glycoforms in which each molecular species contains the conserved phosphoethanolamine-substituted triheptosyl inner-core moiety attached via a phosphorylated Kdo linked to the *O*-deacylated lipid A (Structure **1**). Two populations of glycoforms were observed which differed by 123 Da (i.e., a *P*Etn group). As observed earlier, this was consistent with either phosphate or pyrophosphoethanolamine (*PP*Etn) substitution at the C-4 of the Kdo residue.[16,17] Thus abundant quadruply charged ions at *m/z* 609.5, 640.4, 650.0, and 680.9, together with their corresponding triply charged ions at *m/z* 813.0, 853.5, 867.0, and 908.2 indicated the presence of glycoforms with the respective compositions *P*Cho·Hex_2·Hep_3·*P*Etn_1·*P*·Kdo·Lipid A-OH, *P*Cho·Hex_2·Hep_3·*P*Etn_2·*P*·Kdo·Lipid A-OH, *P*Cho·Hex_3·Hep_3·*P*Etn_1·*P*·Kdo·Lipid A-OH and *P*Cho·Hex_3·Hep_3·*P*Etn_2·*P*·Kdo·Lipid A-OH. In addition, quadruply charged ions at *m/z* 608.8 and 639.6, together with their corresponding triply charged ions at *m/z* 811.9 and 853.0 indicated the presence of glycoforms without *P*Cho with the respective compositions Hex_3·Hep_3·*P*Etn_1·*P*·Kdo·Lipid A-OH and Hex_3·Hep_3·*P*Etn_2·*P*·Kdo·Lipid A-OH. A minor quadruply charged ion at *m/z* 723.0 was observed which was attributed to a sialylated Hex3 glycoform with the corresponding composition Neu5Ac·*P*Cho·Hex_3·Hep_3·*P*Etn_1·*P*·Kdo·Lipid A-OH. Traces of a quadruply charged ion corresponding to Neu5Ac·*P*Cho·Hex_3·Hep_3·*P*Etn_2·*P*·Kdo·Lipid A-OH were observed at *m/z* 753.6. Although of very low abundance, the presence of sialylated glycoforms could be confirmed by ESI tandem-mass spectrometry following on-line separation by capillary electrophoresis (CE-ESIMS/MS). Thus *m/z* 290 corresponding to Neu5Ac was chosen as the fragment ion in a precursor ion-scan experiment. The resulting spectrum (negative mode) is shown in Fig. 1(A). It revealed triply charged ions at *m/z* 964 and 1005 corresponding to the above mentioned glycoforms Neu5Ac·*P*Cho·Hex_3·Hep_3·

Table 1
Linkage analysis data for LPS derived samples from *H. influenzae* NTHi strain 176

Methylated sugar [a]	T_{gm} [b]	Relative detector response				Linkage assignment
		LPS	LPS-P [c]	OS-1	OS-2	
2,3,4,6-Me_4-Glc	1.00	22	13	27	33	D-Glc*p*-(1-
2,3,4,6-Me_4-Gal	1.04	17	10	23	19	D-Gal*p*-(1-
2,3,6-Me_3-Glc	1.17	7	14	0.5	13	-4)-D-Glc*p*-(1-
2,4,6-Me_3-Gal	1.18	6	1	0.5	1	-3)-D-Gal*p*-(1-
2,3,4-Me_3-Glc	1.19		1	1		-6)-D-Glc*p*-(1-
2,3,4,6,7-Me_5-Hep	1.28	2	1	5	2	L,D-Hep*p*(1-
2,3,-Me_3-Glc	1.33		1	2		-4,6)-D-Glc*p*-(1-
3,4,6,7-Me_4-Hep	1.41	2	12			-2)-L,D-Hep*p*(1-
2,4,6,7-Me_4-Hep	1.43	19	12	21	14	-3)-L,D-Hep*p*(1-
2,6,7-Me_3-Hep	1.47	22	26	20	17	-3,4)-L,D-Hep*p*-(1-
4,6,7-Me_3-Hep	1.54		8		1	-2,3)-L,D-Hep*p*-(1-
2,3,4,-Me_4-GlcN	1.68	2	2			-6)-D-Glc*p*NAc(1-

[a] 2,3,4,6-Me_4-Glc represents 1,5-di-*O*-acetyl-2,3,4,6-tetra-*O*-methyl-D-glucitol-1-d_1, etc.
[b] Retention times (T_{gm}) are reported relative to 2,3,4,6-Me_4-Glc.
[c] LPS treated with aq HF prior methylation analysis.

Table 2
Negative ion ESIMS data and proposed compositions for *O*-deacylated LPS (LPS-OH) and oligosaccharide preparations OS-1 and OS-2 of non-typeable *H. influenzae* strain 176

Sample	Observed ions (m/z)			Molecular mass (Da)		Relative abundance (%)	Proposed composition
	$[M-4H]^{4-}$	$[M-3H]^{3-}$	$[M-2H]^{2-}$	Observed	Calculated		
LPS-OH	608.8	811.9		2439.0	2439.2	7	$Hex_3{\cdot}Hep_3{\cdot}PEtn_1{\cdot}P_1{\cdot}Kdo_1{\cdot}$LipidA-OH
	609.5	813.0		2442.0	2442.2	7	$PCho{\cdot}Hex_2{\cdot}Hep_3{\cdot}PEtn_1{\cdot}P_1{\cdot}Kdo_1{\cdot}$LipidA-OH
	639.6	853.0		2562.2	2562.3	9	$Hex_3{\cdot}Hep_3{\cdot}PEtn_2{\cdot}P_1{\cdot}Kdo_1{\cdot}$LipidA-OH
	640.4	853.5		2564.6	2565.3	8	$PCho{\cdot}Hex_2{\cdot}Hep_3{\cdot}PEtn_2{\cdot}P_1{\cdot}Kdo_1{\cdot}$LipidA-OH
	650.0 [a]	867.0 [a]		2604.0	2604.3	29	$PCho{\cdot}Hex_3{\cdot}Hep_3{\cdot}PEtn_1{\cdot}P_1{\cdot}Kdo_1{\cdot}$LipidA-OH
	680.9 [a]	908.2 [a]		2727.6	2727.3	38	$PCho{\cdot}Hex_3{\cdot}Hep_3{\cdot}PEtn_2{\cdot}P_1{\cdot}Kdo_1{\cdot}$LipidA-OH
	723.0	[b]		2895.5	2895.6	2	$Neu5Ac{\cdot}PCho{\cdot}Hex_3{\cdot}Hep_3{\cdot}PEtn_1{\cdot}P_1{\cdot}Kdo_1{\cdot}$LipidA-OH [c]
OS-1			704.4	1410.8	1411.1	14	$PCho{\cdot}Hex_2{\cdot}Hep_3{\cdot}PEtn_1{\cdot}An$Kdo-ol
			733.0	1468.0	1468.2	5	$PCho{\cdot}Gly{\cdot}Hex_2{\cdot}Hep_3{\cdot}PEtn_1{\cdot}An$Kdo-ol
			785.4	1572.8	1573.3	56	$PCho{\cdot}Hex_3{\cdot}Hep_3{\cdot}PEtn_1{\cdot}An$Kdo-ol
			814.0	1630.0	1630.4	22	$PCho{\cdot}Gly{\cdot}Hex_3{\cdot}Hep_3{\cdot}PEtn_1{\cdot}An$Kdo-ol
			842.7	1687.4	1687.4	3	$PCho{\cdot}Gly_2{\cdot}Hex_3{\cdot}Hep_3{\cdot}PEtn_1{\cdot}An$Kdo-ol
OS-2			621.9	1245.8	1246.0	7	$Hex_2{\cdot}Hep_3{\cdot}PEtn_1{\cdot}An$Kdo-ol
			650.4	1302.8	1303.2	2	$Gly{\cdot}Hex_2{\cdot}Hep_3{\cdot}PEtn_1{\cdot}An$Kdo-ol
			702.9	1407.8	1408.1	36	$Hex_3{\cdot}Hep_3{\cdot}PEtn_1{\cdot}An$Kdo-ol
			731.4	1464.8	1465.3	13	$Gly{\cdot}Hex_3{\cdot}Hep_3{\cdot}PEtn_1{\cdot}An$Kdo-ol
			784.0	1570.0	1570.2	32	$Hex_4{\cdot}Hep_3{\cdot}PEtn_1{\cdot}An$Kdo-ol
			812.4	1626.8	1627.4	10	$Gly{\cdot}Hex_4{\cdot}Hep_3{\cdot}PEtn_1{\cdot}An$Kdo-ol

Average mass units were used for calculation of molecular-weight values based on proposed compositions as follows: Hex, 162.14; Hep, 192.17; Kdo, 220.18; *An*Kdo-ol, 222.20; *P*, 79.98; *P*Etn, 123.05, *P*Cho, 165.13; Neu5Ac, 291.26; Gly, 57.05 and lipid A-OH, 953.02. Relative abundance was estimated from the area of the ion peaks relative to the total area (expressed as percentage). Peaks representing less than 5% of the base peak are not included in the table.

[a] Peak shape analysis indicates possible contributions to the signal area from quadruply (641.3/680.2) and triply (866.0/907.2) charged ions corresponding to $Hex_4{\cdot}Hep_3{\cdot}PEtn_{1,2}{\cdot}P_1{\cdot}Kdo_1{\cdot}$LipidA-OH.

[b] Not detected

[c] Traces of an ion corresponding to $Neu5Ac{\cdot}PCho{\cdot}Hex_3{\cdot}Hep_3{\cdot}PEtn_2{\cdot}P_1{\cdot}Kdo_1{\cdot}$LipidA-OH was observed at m/z 753.6.

$PEtn_{1,2}{\cdot}P_1{\cdot}Kdo_1{\cdot}$LipidA-OH. In this experiment, additional minor ions at m/z 1061 and 1103 were observed corresponding to disialylated glycoforms with respective compositions $Neu5Ac_2{\cdot}PCho{\cdot}Hex_3{\cdot}Hep_3{\cdot}PEtn_{1,2}{\cdot}P_1{\cdot}Kdo_1{\cdot}$LipidA-OH. The ions at m/z 1061 and 1103 were further fragmented in MS/MS experiments, and the corresponding product ion spectra revealed, inter alia, a fragment ion at m/z 581 indicating a Neu5Ac disaccharide unit in the corresponding glycoforms. This was confirmed by further fragmenting m/z 581 in a MS^3 experiment producing only fragment ions due to loss/addition of Neu5Ac (Fig. 1(B)).

Characterization of major core oligosaccharide fractions.—Partial-acid hydrolysis of LPS with dilute acetic acid afforded an insoluble lipid A and core oligosaccharide fractions which were separated by GPC (see Section 4) to give two major fractions, OS-1 and OS-2. The methylation analyses data for OS-1 and OS-2 are presented in Table 1. Methylation analysis of OS-1 showed terminal Glc, terminal Gal, 4-substituted Glc, 3-substituted-Hep, and 3,4-disubstituted Hep as the major sugar components. Methylation analysis of OS-2 showed in addition to those observed in OS-1, 4-substituted Glc. The ESIMS spectrum of OS-1 (see Table 2)

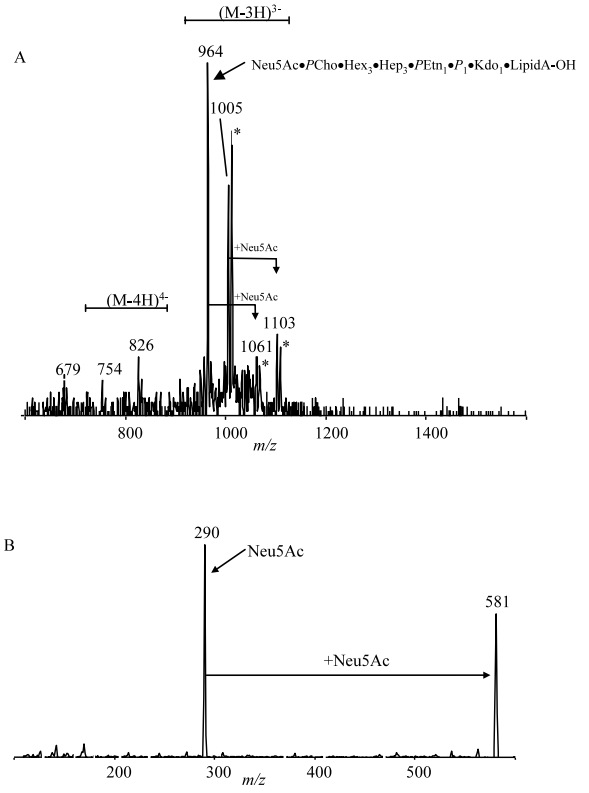

Fig. 1. CE-ESIMS/MS (negative mode) spectra of LPS-OH derived from NTHi 176. (A) Precursor ion spectrum using m/z 290 as the fragment ion for identification of sialylated components. Ions indicated with asterisk (*) correspond to sodiated adducts. The ion at m/z 1005 corresponds to *P*Cho·Neu5Ac·Hex_3·Hep_3·*P*Etn_2·*P*·Kdo·Lipid A-OH. The ion at m/z 679 is not rationalized. (B) MS/MS spectrum of fragment ion m/z 581 promoted using an orifice voltage of 180V. The fragmentation pattern is indicated.

showed major doubly charged ions at m/z 704.4, 733.0, 785.4 and 814.0 corresponding to glycoforms with composition *P*Cho·Hex_2·Hep_3·*P*Etn_1·*An*Kdo-ol, *P*Cho·Gly·Hex_2·Hep_3·*P*Etn_1·*An*Kdo-ol, *P*Cho·Hex_3·Hep_3·*P*Etn_1·*An*Kdo-ol and *P*Cho·Gly·Hex_3·Hep_3·*P*Etn_1·*An*Kdo-ol. A very minor ion at m/z 842.7 might suggest the presence of a Hex3 glycoform containing two glycine residues. The ESIMS for OS-2 showed major ions at m/z 702.9, 731.4, 784.0, and 812.4 which corresponded to glycoforms with the respective compositions Hex_3·Hep_3·*P*Etn·*An*Kdo-ol, Gly·Hex_3·Hep_3·*P*Etn·*An*Kdo-ol, Hex_3·Hep_3·*P*Etn·*An*Kdo-ol and Gly·Hex_4·Hep_3·*P*Etn·*An*Kdo-ol. In addition, minor ions at m/z 621.9 and 650.4 corresponded to glycoforms with the respective compositions Hex_2·Hep_3·*P*Etn·*An*Kdo-ol and Gly·Hex_2·Hep_3·*P*Etn·*An*Kdo-ol. It was obvious that OS-1 contained glycoforms with *P*Cho and OS-2 was composed of glycoforms lacking *P*Cho. Information on the location of Gly, as well as glycose sequence of the *P*Cho·Hex_3·Hep_3·*P*Etn·*An*Kdo-ol component was provided by CE-ESIMS/MS in the positive mode. The product ion spectrum obtained from its doubly charged ion at m/z 788 is shown in Fig. 2(A). The ions at m/z 1219 and 1084 corresponded to losses of HexHep and HexHex*P*Cho units from the molecular ion, respectively. In addition, the doubly charged ion at m/z 706 corresponded to the loss of one hexose unit. To confirm it's basic structure, this ion was further fragmented in an MS^3 experiment (Fig. 2(B)). The resulting product ion spectrum was dominated by the ion at m/z 316 corresponding to Hep*P*Etn to which an addition of Hep resulted in m/z 508. The ion at m/z 328 corresponded to *P*ChoHex to which additions corresponding to Hex (m/z 490) or Hep (m/z 520) could be made, the latter giving evidence for that *P*ChoHex substituted HepI. The ion at m/z 904 corresponded to a composition *P*Cho·Hex_2·Hep·*An*Kdo-ol from which consecutive losses corresponding to *An*Kdo-ol (m/z 682) and Hep (m/z 490) or Hex (m/z 520) could be made. These results strongly indicated the basic structure for the Hex3 glycoform shown in Fig. 2(A). The product ion spectrum (positive mode) obtained from the doubly charged ion at m/z 816 (composition *P*Cho·Gly·Hex_3·Hep_3·*P*Etn·*An*Kdo-ol), and its proposed fragmentation pattern is shown in Fig. 2(C). As observed earlier,[15] the marker ion at m/z 251 corresponded to HepGly to which an addition corresponding to Hex (m/z 413) could be made giving evidence for Gly substituting HepIII.

Characterization of OS-1 and OS-2 by NMR spectroscopy.—The ^{1}H NMR spectra were assigned using chemical shift correlation techniques (COSY and TOCSY experiments) and the chemical shift data are presented in Table 3. Subspectra corresponding to the individual glycosyl residues were identified on the basis of spin-connectivity pathways delineated in the ^{1}H chemical shift correlation maps, the chemical shift values, and the vicinal coupling constants. The chemical shift data are consistent with each D-sugar residue being present in the pyranosyl ring form. Further evidence for this conclusion was obtained from NOE data (Table 4) which also served to confirm the anomeric configurations of the linkages and the monosaccharide sequence. The Hep ring systems were identified on the basis of the small $J_{1,2}$-values and their α configurations were confirmed by the occurrence of single intraresidue NOE between the respective H-1 and H-2 resonances. The occurrence of transglycosidic NOEs (Table 4) between the proton pairs HepIII H-1/HepII H-1,2, HepII H-1/HepI H-3 in OS-1 and OS-2 confirmed the sequence of the heptose-containing trisaccharide unit L-α-D-Hep*p*-(1→2)-[*P*Etn→6]-L-α-D-Hep*p*-(1→3)-L-α-D-Hep*p*-(1→. Several signals for methylene protons of *An*Kdo-ol were observed in the COSY and TOCSY spectra in the region 2.25–1.65. This is due to the fact that several anhydro-forms of Kdo are formed during the hydrolysis as observed earlier.[1]

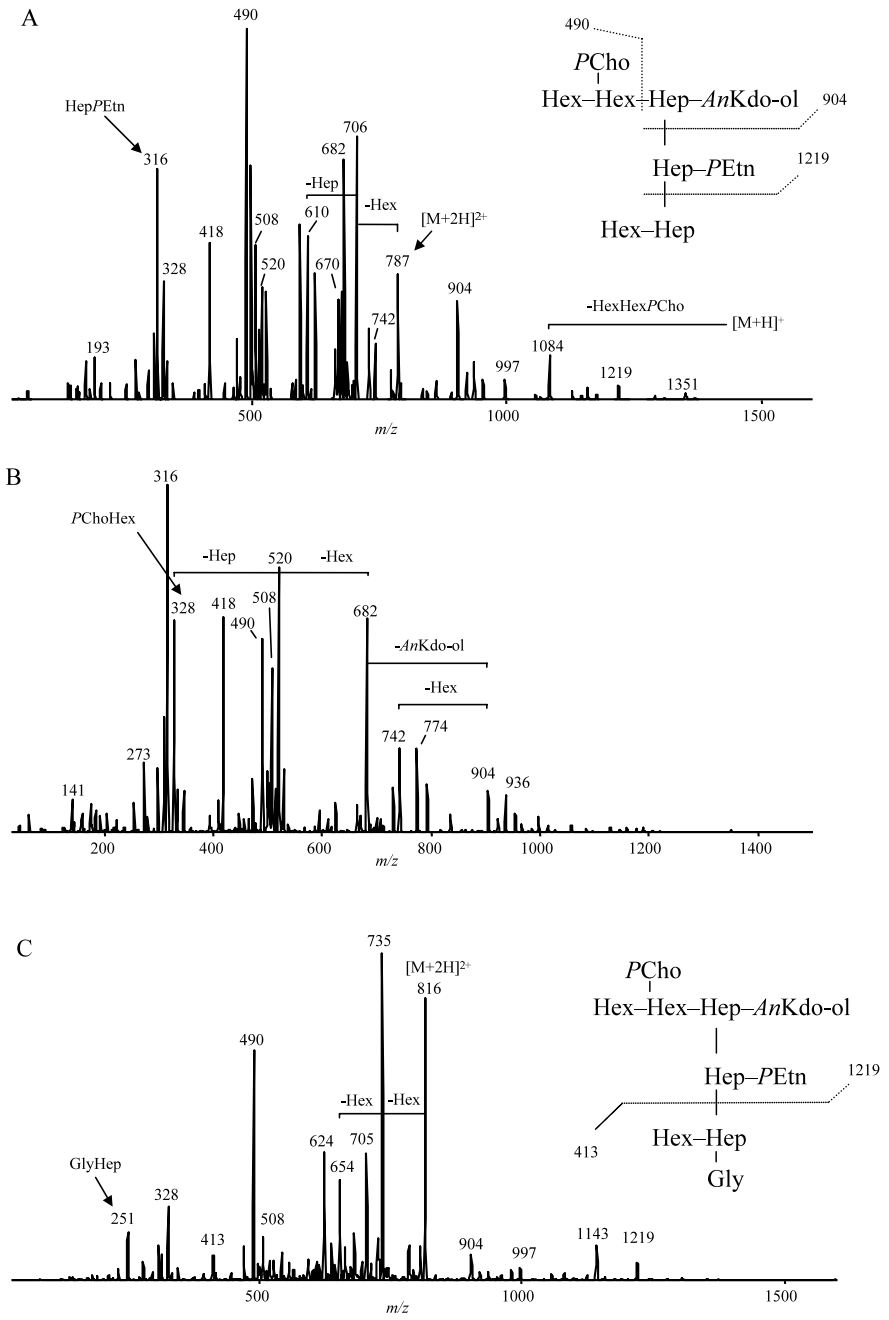

Fig. 2. CE-ESIMS/MS (positive mode) spectra of glycoforms observed in OS-1 derived from *H. influenzae* non-typeable strain 176. Selected ions of structural significance are indicated. (A) Product ion spectrum of $[M+2H]^{2+}$ m/z 788 (composition *P*Cho·Hex_3·Hep_3·*P*Etn·*An*Kdo-ol) and its proposed fragmentation pattern. (B) MS/MS spectrum of fragment ion m/z 706 (MS^3) promoted using an orifice voltage of 180 V. (C) Product ion spectrum of $[M+2H]^{2+}$ m/z 816 (composition *P*Cho·Gly·Hex_3·Hep_3·*P*Etn·*An*Kdo-ol) and its proposed fragmentation pattern.

Hex2 and Hex3 glycoforms containing PCho. The structure of the Hex3 glycoform in OS-1 could be determined by examining the ^{1}H NMR spectrum (Fig. 3(A)) in detail. The characteristic signal for the methyl groups of *P*Cho was observed at δ 3.24. Anomeric resonances of HepI–HepIII were identified at δ 5.03–5.13, 5.83 and 5.26, respectively. Subspectra corresponding to GlcI, GlcII, and Gal were identified in the 2D COSY and TOCSY spectra at δ 4.56, 4.62 and 4.64, respectively. Chemical shift data are consistent with GlcII and Gal being terminal residues in agreement with methylation analyses. From the downfield shifted H-6_A,6_B of GlcI at δ 4.30, it was concluded that this residue was substituted with *P*Cho at this position which was in agreement with CE-ESIMS/MS analyses (Fig. 1). Interresidue NOE connectivities between pro-

ton pairs GlcII H-1/GlcI H-4, GlcI H-1/HepI H-4,6 (Table 4) established the sequence of a disaccharide unit and its attachment point to HepI as β-D-Glc*p*-(1→4)-[*P*Cho→6]-β-D-Glc*p*-(1→4)-L-α-D-Hep*p*-(1→. Interresidue NOE between H-1 of Gal and H-3/H-2 of HepIII gave evidence for the a β-D-Gal*p*-(1→3)-L-α-D-Hep*p*-(1→ unit. From the combined data it could thus be concluded that the *P*Cho substituted Hex3 glycoform has structure **2**. Methylation analysis of OS-1 (Table 1) showed a significant amount of terminal Hep and it was concluded that the *P*Cho substituted Hex2 glycoform observed in ESIMS spectra has structure **3**. The spin system due to HepIII of this component could not be definitively assigned because of the relative minor amounts in the sample. As mentioned above, Gly partly substitutes all glycoforms at HepIII as evidenced from CE-ESIMS/MS.

*P*Cho
↓
6
β-D-Glc*p*-(1→4)-β-D-Glc*p*-(1→4)-L-α-D-Hep*p*-(1→5)-*An*Kdo-ol
3
↑
1
L-α-D-Hep*p*6←*P*Etn
2
↑
1
R→3)-L-α-D-Hep*p*---Gly

2. R = β-D-Gal*p*(1

3. R = OH

Hex3 and Hex4 glycoforms lacking PCho.—The ^{1}H NMR spectrum of OS-2 is shown in Fig. 3(B). In agreement with ESIMS data, glycoforms containing the *P*Cho substituent are not significantly present as in OS-1 since the signal for methyl protons of *P*Cho (δ 3.24) is only minor. Signals for anomeric protons of HepI–HepIII resonate at approximately identical chemical shifts as the corresponding ones in OS-1 (Table 3). At δ 5.26, the anomeric resonance of an α-linked terminal Glc residue (GlcIII) is observed. The anomeric region for β-linked hexoses was more complex than in OS-1 due to higher heterogeneity of the sample. In 2D spectra, two spin systems for the terminal GlcII were observed at δ 4.50 and 4.45. The 4-substituted GlcI and two spin systems for the terminal Gal residues were identified at δ 4.56, 4.61 and 4.54. NOE data confirmed the presence of the structural element β-D-Glc*p*-(1→4)-β-D-Glc*p*-(1→4)-L-α-D-Hep*p*-(1→, as well as the occurrence of the β-D-Gal, linked to HepIII. Since methylation analysis on LPS-*P* showed increased 2,3-substituted Hep, it was concluded that the α-linked Glc was linked to the 3-position of HepII which was

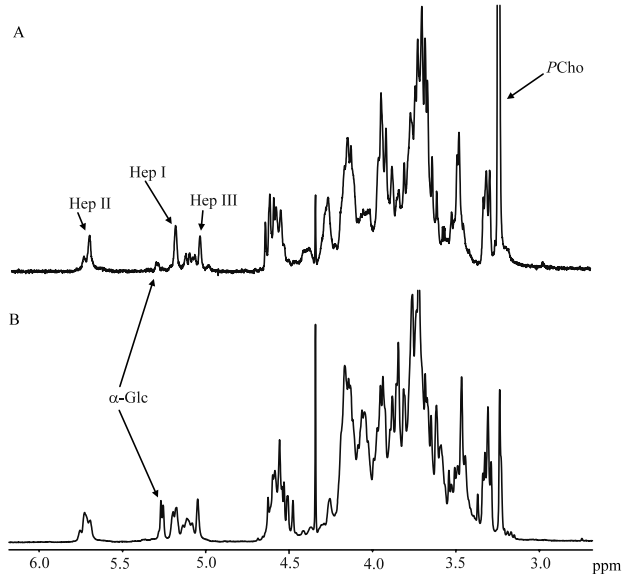

Fig. 3. 270 MHz ^{1}H NMR spectra of OS-1 (A) and OS-2 (B) derived from *H. influenzae* non-typeable strain 176 in D_2O at 70 °C.

corroborated by NOE connectivities between H-1 of the α-linked Glc residue to δ 4.04 tentatively assigned to H3 of HepII. The combined evidence lead to the structure of the Hex4 glycoform as shown in **4**. In agreement with methylation analysis showing terminal Hep, the predominant Hex3 glycoform most likely has the structure **5**. It is concluded that Gly partly substitutes all glycoforms at HepIII as evidenced from CE-ESIMS/MS (see above).

β-D-Glc*p*-(1→4)-β-D-Glc*p*-(1→4)-L-α-D-Hep*p*-(1→5)-*An*Kdo-ol
3
↑
1
α-D-Glc*p* →3)-L-α-D-Hep*p*6←*P*Etn
2
↑
1
R_1→3)-L-α-D-Hep*p*---Gly

4. R_1 = β-D-Gal*p*

5. R_1 = OH

3. Discussion

NTHi strain 176 is an isolate obtained from a child with otitis media as part of an epidemiological study in Finland. Previous studies of LPS from *H. influenzae* have resulted in a structural model consisting of a conserved L-*glycero*-D-*manno*-heptose-containing trisaccharide inner-core attached via a phosphorylated Kdo unit to the lipid A moiety (Structure **1**). The results of the present study confirm the presence of this structural element in NTHi strain 176. In the major

Table 3
^{1}H and chemical shifts for oligosaccharide preparations OS-1 and OS-2 derived from *H. influenzae* non-typeable strain 176

Sample	residue	glycose unit	H-1	H-2	H-3	H-4	H-5	H-6$_A$	H-6$_B$	H-7$_A$	H-7$_B$
OS-1	HepI	→3,4)-L-α-D-Hep*p*-(1→	5.13-5.03[a]	4.06-3.98[a]	4.06-3.98[a]	4.32[b]	-[c]	4.12[b]		-	-
			(n.r.)								
	HepII	→2)-L-α-D-Hep*p*-(1→ 6 ↑ *P*Etn	5.83	4.28	3.92	4.17	-	4.56		3.70	3.90
	HepIII[d]	→3)-L-α-D-Hep*p*(1→	5.26	4.28	4.15	3.92	3.84	-		-	-
			(n.r.)								
	GlcI	→4)-β-D-Glc*p*-(1→ 6 ↑ *P*Cho	4.56	3.51	3.60	3.73	3.70	4.30	4.30		
			(7.4)								
	GlcII	β-D-Glc*p*-(1→	4.62	3.26	3.49	3.49	3.49	3.77	3.87		
			(7.6)								
	GalI	β-D-Gal*p*-(1→	4.64	3.59	3.68	3.92	3.68[e]	-	-		
			(7.6)								
	*P*Etn		4.14	3.28							
	*P*Cho		4.39	3.70							
OS-2	Hep I	→3,4)-L-α-D-Hep*p*-(1→	5.12-5.03	4.03-3.97[a]	4.03-3.97[a]	4.33[b]	-	4.09[b]		-	-
			(n.r.)								
	HepII	→2,3)-L-α-D-Hep*p*(1→ 6 ↑ *P*Etn	5.82	4.28	4.04[e]	-	-	-		-	-
			(n.r.)								
	HepIII[f]	→3)-L-α-D-Hep*p*(1→	5.26	4.13	4.27[e]	-	-	-		-	-
			(n.r.)								
			5.24	4.02	4.21[e]	-	-	-		-	-
			(n.r.)								

Table 3 (*Continued*)

GlcI	→4)-β-D-Glc*p*-(1→	4.56	3.45	≈3.60	≈3.60	≈3.60	3.87	4.04
		(7.6)						
GlcII	β-D-Glc*p*-(1→	4.45	3.32	3.48	3.41	3.48	3.77	3.87
		(7.2)						
		4.50	3.32	3.48	3.48	3.48	3.77	3.87
		(7.6)						
Glc III	α-D-Glc*p*-(1→	5.26	3.54	3.74	3.87	-	-	-
		(n.r.)						
Gal	β-D-Gal*p*-(1→	4.61	3.59	3.68	3.92	-	-	-
		(7.6)						
		4.54	3.59	3.69	3.92	-	-	-
		(7.6)						
*P*Etn		3.28	4.13					

Data was recorded in D_2O at 25 °C. $^3J_{H,H}$ values for anomeric ^1H resonances (H-1) are given in parentheses; n.r., not resolved (small coupling). Pairs of deoxy protons of reduced, *An*Kdo were identified in the DQF-COSY at 2.25–1.65 ppm. The signal corresponding to *P*Cho methyl protons occurred at 3.24 ppm.

[a] Several signals were observed for HepI and HepII due to heterogeneity in the *An*Kdo moiety.

[b] H-4/H-6 of HepI are observed by NOE from H-1 of GlcI.

[c] –, Not obtained.

[d] Signals for this residue in **3** (t-Hep) were not identified due to low sensitivity.

[e] tentative assignment from NOE data.

[f] Signals for this residue in **5** (t-Hep) were not identified due to low sensitivity.

glycoform population of this strain, HepI is found to be substituted by a cellobiose unit (Structure **1**; R_1 = β-D-Glc*p*-(1→4)-β-D-Glc*p*). In about 60% of the glycoforms the 4-substituted glucose of this unit carries a *P*Cho at O-6. HepII is either unsubstituted or substituted by a glucose residue (R_2 = α-D-Glc*p*) and HepIII is substituted by galactose (R_3 = β-D-Gal*p*) at O-3. Substitution at O-3 of HepIII was recently and for the first time observed for NTHi strain 486.[1] However, in strain 486, HepIII is substituted by glucose (R_3 = β-D-Glc*p*). In NTHi strain 176, subpopulations of glycoforms were also found in which HepIII was unsubstituted. The *P*Cho epitope is a common feature in the LPS of *H. influenzae*. To date, it has been found to substitute terminal glycose residues linked to HepI (Structure **1**; R_1 = *P*Cho→6)-β-D-Glc*p*, strain Rd$^-$, NTHi strain 1003)[17,18], HepII (Structure **1**; R_2 = *P*Cho→6)-α-D-Glc*p*, NTHi 486)[1] and HepIII (Structure **1**; R_3 = *P*Cho→6)-β-D-Gal*p*, *H. influenzae* type b strains).[11] Substitution with *P*Cho at a branched position has recently been found in NTHi strain SB33 (Structure **1**; R_1 = β-D-Glc*p*-(1→4)-[*P*Cho→6]-β-D-Glc*p*).[19] The expression and phase variation of the *P*Cho epitope on the *H. influenzae* LPS require the four genes of the *lic1* locus.[8] The ability of this organism to link *P*Cho to different oligosaccharide components was recently demonstrated to be associated with DNA sequence polymorphisms in *lic1D*, a gene encoding a putative diphosphonucleoside choline transferase.[20] It is noteworthy that glycoforms having a *P*Cho substituted cellobiose unit are unsubstituted at HepII indicating possible steric interference to glycan addition of HepII during LPS biosynthesis. It is possible that this is coupled to phase variation of *P*Cho expression.

Table 4
Proton NOE data for oligosaccharide preparation OS-1 and OS-2 derived from LPS of NT *H. influenzae* strain 176

Anomeric proton	Observed proton	
	Intraresidue NOE	Interresidue NOE
HepI	H-2	NR [a]
HepII	H-2	H-3 of HepI; H-1 of HepIII [b]
HepIII	H-2	H-1, H-2 of HepII [b]
GlcI	H-3, H-5	H-4, H-6 of HepI
GlcII	H-3, H-5	H-4 of GlcI
GlcIII [c]	H-2	H-3 of HepII
Gal [c]	H-3, H-5	H-2, H-3 of HepIII

Measurements were made from NOESY experiments.
[a] NR, not rationalized.
[b] This signal was not observed in OS-2 due to low sensitivity.
[c] Observed only in the spectrum of OS-2.

Earlier investigations have shown that modification of the LPS with Neu5Ac is widespread among *H. influenzae* strains but few structural investigations of sialylated *H. influenzae* LPS have been reported.[21,22] However, in strains which express sufficient amounts of Neu5Ac containing glycoforms, structural details have been established. *H. influenzae* strain Rd[11] and NTHi strains 486[1], 375,[22] and 1003[18] have been found to express sialylated glycoforms with Neu5Ac linked to the β-galactose of a lactose moiety (Structure **1**; $R_3 = \alpha$-Neu5Ac-(2→3)-β-D-Gal*p*-(1→4)-β-D-Glc*p*). In addition, very minor components comprising two Neu5Ac residues were observed in strains 375 and 1003. Recently, the Neu5Ac level in LPS from 24 different NTHi strains was determined by HPAEC.[14] Using CE-ESIMS/MS methods here, we found that NTHi 176 LPS expresses low levels of sialylated and disialylated Hex3 glycoforms. In addition, the disialylated glycoforms were proven to contain a Neu5Ac disaccharide unit. Sialic acid expression in *H. influenzae* LPS has been shown to be dependent on growth conditions[12,23] and in some strains it has been demonstrated that an exogenous source of Neu5Ac is required for optimal expression.[12] The complete structure of the sialylated glycoforms in NTHi strain 176 is under investigation.

4. Experimental

Bacterial cultivation and preparation of LPS.—*H. influenzae* non-typeable strain 176 was obtained from the strain collection from Professor Eskola as part of a Finnish otitis media cohort study, as isolate obtained from the middle ear. Bacteria were grown in brain heart infusion (BHI) broth (Difco) (3.7%, w/v) containing nicotinamide adenine dinucleotide (NAD) (2 μg/mL), hemin (10 μg/mL) and neuraminic acid (Neu5Ac; 10 μg/mL) at 37 °C. The bacterial growth was harvested and the LPS extracted from lyophilized bacteria by using the phenol–$CHCl_3$–petroleum ether method involving precipitation of the LPS with 1:5 Et_2O–acetone (6 vols.) as described earlier.[1]

Chromatography.—Gel permeation chromatography (GPC) was performed using a Bio-Gel P4 column (2.6 × 140 cm) with pyridinium acetate (0.05 M, pH 4.5, respectively) as eluent. Column eluents were monitored by using a differential refractometer and fractions were collected by lyophilization. Gas liquid chromatography (GLC) was carried out using a Hewlett–Packard 5890 instrument with a DB-5 fused silica capillary column [25 m × 0.25 mm (0.25 μm i.d.)] and a temperature gradient of 160 °C (1min) →250 °C at 3 °C/min.

Preparation of oligosaccharides

O-*Deacylation of LPS with hydrazine*. *O*-Deacylation of LPS was achieved as previously described.[24] Briefly, LPS (5 mg) was mixed with anhyd hydrazine (0.5 mL) and stirred at 37 °C for 1 h. The reaction mixture was cooled and cold acetone (5 mL) was added to destroy excess hydrazine. The precipitated *O*-deacylated LPS (LPS-OH) was centrifuged (48,200*g*, 20 min), the pellet was washed twice with cold acetone, once with Et_2O, and then dissolved in water followed by lyophilization.

Mild-acid hydrolysis of LPS. Core oligosaccharide fractions were obtained from LPS (50 mg) following mild-acid hydrolysis (1% AcOH, pH 3.1, 100 °C, 2 h). The insoluble lipid A (16.2 mg) was separated from the hydrolysis mixtures by centrifugation. The reducing agent, borane-*N*-methylmorpholine complex, was included in the hydrolysis mixture, and, following purification by GPC on the Biogel P4 column, three oligosaccharide fractions, Fr.1 (leading, 1.2 mg), Fr.2 (6.2 mg) and Fr.3 (3.9 mg) were obtained. Fr.2 and Fr.3 were subjected to a second purification on the Biogel P4 column resulting in OS-1 and OS-2, respectively, which were investigated in this study.

Dephosphorylation. LPS (2mg) was incubated with 48% hydrogen fluoride (0.2 mL) for 48 h at 4 °C. Then, the sample was placed into an ice bath and HF was evaporated under a stream of nitrogen gas. The sample, LPS-P, was dissolved in water and lyophilized.

Analytical methods.—Sugars were identified as their alditol acetates as previously described.[25] Methylation analysis was accomplished on acetylated material which was obtained by treatment of the oligosaccharides with Ac_2O (0.5 mL) and 4-diethylaminopyridine (0.5 mg) at rt for 24 h. Methylation was then performed with methyl iodide in dimethylsulfoxide in the presence of lithium methylsulfinylmethanide.[26] The methylated compounds were recovered using a SepPak C18

cartridge and subjected to sugar analysis. The relative proportions of the various alditol acetates and partially methylated alditol acetates obtained in sugar and methylation analyses, discussed below, correspond to the detector response of the GLC–MS. The absolute configuration of glycoses was determined by the method devised by Gerwig et al.[27]

Mass spectrometry.—Electrospray ionization mass spectrometry (ESIMS) was recorded on a VG Quattro triple quadrupole mass spectrometer (Micromass, Manchester, UK) in the negative ion mode. LPS-OH and OS samples were dissolved in a mixture of 1:1 water–MeCN. Sample solutions were injected via a syringe pump into a running solvent of 1:1 water–MeCN at a flow rate of 10 μL/min. CE-ESIMS and CE-ESIMS/MS was carried out with a crystal model 310 CE instrument (AYI Unicam, Boston, MA, USA) coupled to an API 3000 mass spectrometer (Perkin–Elmer/Sciex, Concord, Canada) via a MicroIonspray interface using 15 mM ammonium acetate–ammonium hydroxide in deionized waster, pH 9.0, containing 5% MeOH as running solvent. Mass spectra were acquired with dwell times of 3.0 ms per step of 1 m/z unit in full-mass scan mode. The MS/MS data were acquired in full-scan mode using a dwell time of 2.0 ms per step of 1 m/z unit which leads to the mass precision of $+1$ Da. Fragment ions formed by collision activation of selected precursor ions with nitrogen in the RF-only quadrupole collision cell, were mass-analyzed by scanning the third quadrupole. In the triple quadrupole mass spectrometer, only MS^2 or MS/MS is normally used for structural analysis. However, when the potential between the orifice plate and the skimmer is high enough, fragmentation can then take place. This method of collision induced dissociation (CID) is referred to as front end CID. In combination with the front-end CID, we are able to obtain an MS/MS spectrum of a fragment ion or MS,[3] which was generated using an orifice voltage. In this study, the potential between the orifice plate and the skimmer was increased from 60 to 180 V for MS^3 experiments. The precursor-ion spectra were obtained by selecting the fragment ions in the third quadrupole and mass scan the first quadrupole. The recorded spectrum corresponds to the ions that could give rise to the selected fragment ions (precursor). In the current study, m/z 290 was chosen as the fragment ion for identification of sialylated LPS. GLC–MS was carried out with a Delsi Di200 chromatograph equipped with a NERMAG R10-10H quadrupole mass spectrometer using the same conditions for GLC as described above.

NMR spectroscopy.—NMR spectra were recorded on solutions in deuterium oxide at 25 or 70 °C after several lyophilizations with D_2O. Spectra were acquired on JEOL Esquire 500 and JEOL EX 270 spectrometers using standard-pulse sequences for two-dimensional (2D) COSY, TOCSY, and NOESY experiments. Mixing times of 50 and 180 and 400ms were used for 500 MHz 2D TOCSY and NOESY experiments, respectively. Chemical shifts are reported in ppm, referenced to sodium 3-trimethylsilylpropanoate-d_4 (δ 0.00, ^{1}H).

Acknowledgements

The authors would like to thank sincerely the members of the Finnish Otitis Media Study Group at the National Public Health Institute in Finland for the provision of NTHi strains from the middle ear fluid, obtained as part of the Finnish Otitis Media Cohort Study. Mary Deadman is acknowledged for culture of NTHi strain 176. Anna-Karin Karlsson is acknowledged for technical assistance. Karolinska Institutet is acknowledged for financial support (KI-fonder).

References

1. Månsson, M; Bauer, S. H. J.; Hood, D. W.; Richards, J. C.; Moxon, E. R.; Schweda, E. K. H. *Eur. J. Biochem.* **2001**, *268*, 2148–2159.
2. Kimura, A.; Hansen, E. J. *Infect. Immun.* **1986**, *51*, 69–79.
3. Weiser, J. N.; Williams, A.; Moxon, E. R. *Infect. Immun.* **1990**, *58*, 3455–3457.
4. Weiser, J. N. *J. Infect. Dis.* **1993**, *168*, 672–680.
5. Weiser, J. N.; Maskell, D. J.; Butler, P. D.; Lindberg, A. A.; Moxon, E. R. *J. Bacteriol.* **1990**, *172*, 3304–3309.
6. Jarosik, G. P.; Hansen, E. J. *Infect. Immun.* **1994**, *62*, 4861–4867.
7. Hood, D. W.; Deadman, M. E.; Jennings, M. P.; Bisercic, M.; Fleischmann, R. D.; Venter, J. C.; Moxon, E. R. *Proc. Natl. Acad. Sci. USA* **1996**, *93*, 11121–11125.
8. Weiser, J. N.; Shchepetov, M.; Chong, S. T. H. *Infect. Immun.* **1997**, *65*, 943–950.
9. High, N. J.; Deadman, M. E.; Moxon, E. R. *Mol. Microbiol.* **1993**, *9*, 1275–1282.
10. Hood, D. W.; Deadman, M. E.; Allen, T.; Masoud, H.; Martin, A.; Brisson, J. R.; Fleischmann, R.; Venter, J. C.; Richards, J. C.; Moxon, E. R. *Mol. Microbiol.* **1996**, *22*, 951–965.
11. Schweda, E. K. H.; Brisson, J.-R.; Alvelius, G.; Martin, A.; Weiser, J. N.; Hood, D. W.; Moxon, E. R.; Richards, J. C. *Eur. J. Biochem.* **2000**, *267*, 3902–3913.
12. Hood, D. W.; Cox, A. D.; Gilbert, M.; Makepeace, K.; Walsh, S.; Deadman, M. E.; Cody, A.; Martin, A.; Månsson, M.; Schweda, E. K. H.; Brisson, J.-R.; Richards, J. C.; Moxon, E. R.; Wakarchuk, W. W. *Mol. Microbiol.* **2001**, *39*, 341–351.
13. Hood, D. W.; Deadman, M.; Cox, A.; Martin, A.; Schweda, E. K. H.; Richards, J. C.; Moxon, E. R. *Glycobiology* **2001**, *11*, 957–967.
14. Bauer, S. H. J.; Månsson, M.; Hood, D. W.; Richards, J. C.; Moxon, E. R.; Schweda, E. K. H. *Carbohydr. Res.* **2001**, *335*, 251–260.
15. Li, J.; Bauer, S. H. J.; Månsson, M.; Richards, J. C.; Schweda, E. K. H. *Glycobiology* **2001**, *11*, 1009–1015.
16. Masoud, H.; Moxon, E. R.; Martin, A.; Krajcarski, D.; Richards, J. C. *Biochemistry* **1997**, *36*, 2091–2103.

17. Risberg, A.; Masoud, H.; Martin, A.; Richards, J. C.; Moxon, E. R.; Schweda, E. K. H. *Eur. J. Biochem.* **1999**, *261*, 171–180.
18. Månsson, M.; Hood, D. W.; Li, J.; Richards, J. C.; Moxon, E. R.; Schweda, E. K. H., *Eur. J. Biochem.*, in press.
19. Cox, A. D.; Masoud, H.; Thibault, P.; Brisson, J.-R.; van der Zwan, M.; Perry, M. B.; Richards, J. C. *Eur. J. Biochem.* **2001**, *268*, 5278–5286.
20. Lysenko, E.; Richards, J. C.; Cox, A. D.; Stewart, A.; Martin, A.; Kapoor, M.; Weiser, J. N. *Mol. Microbiol.* **2000**, *35*, 234–245.
21. Mandrell, R. E.; McLaughlin, R.; Kwaik, Y. A.; Lesse, A.; Yamasaki, R.; Gibson, B.; Spinola, S. M.; Apicella, M. A. *Infect. Immun.* **1992**, *60*, 1322–1328.
22. Hood, D. W.; Makepeace, K.; Deadman, M. E.; Rest, R. F.; Thibault, P.; Martin, A.; Richards, J. C.; Moxon, E. R. *Mol. Microbiol.* **1999**, *33*, 679–692.
23. Vimr, E.; Lichtensteiger, C.; Steenbergen, S. *Mol. Microbiol.* **2000**, *36*, 1113–1123.
24. Holst, O.; Brade, L.; Kosma, P.; Brade, H. *J. Bacteriol.* **1991**, *173*, 1862–1866.
25. Sawardeker, J. S.; Sloneker, J. H.; Jeanes, A. *Anal. Chem.* **1965**, *37*, 1602–1604.
26. Blakeney, A. B.; Stone, B. A. *Carbohydr. Res.* **1985**, *140*, 319–324.
27. Gerwig, G. J.; Kamerling, J. P.; Vliegenthart, J. F. G. *Carbohydr. Res.* **1978**, *62*, 349–357.